Theoretical and Applied Climatology (2021) 145:261–272
https://doi.org/10.1007/s00704-021-03632-x

ORIGINAL PAPER

Anomalous arctic polar vortex-induced spring vegetation variability and lagged productivity responses in China

He Gong[1] · Mei Huang[1] · Zhaosheng Wang[1] · Shaoqiang Wang[1] · Fengxue Gu[2]

Received: 28 December 2020 / Accepted: 20 April 2021 / Published online: 29 April 2021

Abstract

The Arctic polar vortex (APV) system plays an important role in controlling winter and spring atmospheric circulation pattern in China. Here, we evaluate the anomalous APV-induced spring vegetation variability and lagged productivity responses in China. We found that both strong and weak APV conditions have almost equally negative impacts on spring vegetation growth in China, e.g., negative NDVI anomalies occurred in 48.6 and 53.2% of China's vegetated areas under strong and weak APV conditions, respectively. However, large seasonal compensation effects were associated with weak APV conditions, and beneficial lagged vegetation productivity responses occurred in 67.2% of China's vegetated areas, whereas adverse responses occurred in only 32.8% of vegetated areas. Under a strong APV, adverse lagged vegetation productivity responses occurred in 54.5% of China's vegetated areas, whereas beneficial responses occurred in only 45.5% of vegetated areas. The temperature, precipitation, and solar radiation changes caused by anomalous APV-induced changes in circulation patterns are the main reasons for spring vegetation variability. The lagged vegetation productivity responses were attributed to anomalous APV-related precipitation and air temperature anomalies in the following summer and autumn. This improved understanding of the strong links between APV anomalies and vegetation dynamics in China should facilitate early warning of vegetation productivity reductions under anomalous APV conditions.

1 Introduction

The Arctic polar vortex (APV) system covers a large area and features low pressure and cold air moving around the center of the northern pole. This system weakens in summer and strengthens in winter and spring. The variability in the APV system is substantially associated with Arctic amplification, i.e., the greater increase in trends and variability in surface air temperature in the Arctic than in other global regions (Serreze and Barry 2011; Cohen et al. 2014; Zhang et al. 2016). Arctic amplification has been related to significant changes in the transport of heat and water in the Arctic (Serreze et al. 2000; Overland and Wang 2010; Screen and Simmonds 2010; Serreze and Barry 2011) and has also been linked to extreme weather events across the mid-latitudes (Francis and Vavrus 2012; Screen and Simmonds 2013; Walsh 2014; Francis and Skific 2015; Overland et al. 2015; Shepherd 2016; Wang et al. 2017; Cohen et al. 2020). The strength of the APV has changed greatly in response to Arctic amplification in recent decades (Stroeve et al. 2007; Kim et al. 2014), and such variations can exert extensive impacts on major climate oscillations, such as the Arctic Oscillation (AO) and El Niño-Southern Oscillation (ENSO) (Thompson and Wallace 1998; Frauenfeld and Davis 2000) and regional climate, such as the surface air temperature (Zhang et al. 1985), precipitation (Zhang et al. 2006, 2008; Xiong et al. 2012), atmospheric circulation (Liu 1986), and snowstorms (Wang et al. 2008; Yi et al. 2009) in China and cold events in North America and Eurasia (Angell and Korshover 1977; Thompson et al. 2002; Mitchell et al. 2013; Zhang et al. 2016).

Since climate factors, such as temperature, precipitation, and solar radiation, are the most important factors affecting vegetation growth (Peng et al. 2020), anomalous APV-induced changes in climate factors should have a profound influence on the vegetation variability in the northern middle to high latitudes. Although vegetation activities in the

✉ Mei Huang
huangm@igsnrr.ac.cn

[1] National Ecosystem Science Data Center, Key Laboratory of Ecosystem Network Observation and Modeling, Institute of Geographic Sciences and Natural Resources Research, Chinese Academy of Sciences, Beijing 100101, China

[2] Key Laboratory of Dryland Agriculture, Ministry of Agriculture, Institute of Environment and Sustainable Development in Agriculture, Chinese Academy of Agricultural Sciences, Beijing 100081, China

northern high latitudes have been intensively studied (Sturm et al. 2001; Tucker et al. 2001; Tape et al. 2006; Bunn et al. 2007; Bhatt et al. 2010; Pearson et al. 2013), few approaches have focused on the linkage between vegetation dynamics and the APV (Li et al. 2017).

The atmospheric circulation patterns in the spring and winter in China are largely controlled by the APV. Since spring is a critical season for vegetation growth and because spring environmental stresses, such as low temperatures and drought, can easily cause cellular damage in vegetation (Norby et al. 2003; Inouye 2008), APV anomalies in spring should have a great influence on vegetation variability in China. Whether APV-induced spring vegetation variability has negative or positive seasonal compensation effects in the subsequent summer and autumn is another important issue to address. Previous studies have shown that the spring environmental stresses, such as low temperatures and drought lasting several months, can greatly reduce vegetation productivity (Noormets et al. 2008; Hufkens et al. 2012). However, Buermann et al. (2018) demonstrated that contrasting lagged productivity responses to spring environmental change exist widely in northern ecosystems, which indicates that spring vegetation variability may not result in the reduction of vegetation productivity. Therefore, it is important to explore the lagged response of vegetation productivity to anomalous APV conditions and to explore the mechanism.

The satellite-observed normalized difference vegetation index (NDVI) is used as a measure of vegetation growth and vegetation activity and is a proxy for potential photosynthesis (Pinzon and Tucker 2014). In this study, we utilized NDVI data, flux tower observed gross primary productivity (GPP) data, and a spring APV index (APVI) to investigate the anomalous APV-induced spring vegetation variability and lagged vegetation productivity responses in China. The objectives of this study are (Angell and Korshover 1977) to demonstrate the impacts of anomalous APV conditions on spring vegetation variability, (Bao et al. 2014) to estimate the lagged productivity responses, and (Bhatt et al. 2010) to characterize the physical linkage between anomalous APV conditions and China's vegetation variability. This approach is anticipated to provide a more comprehensive understanding of the vegetation variability in China in association with anomalous APV conditions. The results are useful for early warning of the threats of vegetation productivity reduction in response to APV anomalies in China.

2 Data and methods

2.1 Climate data

The monthly mean precipitation and surface air temperature data, covering the period of 1982–2015 at a resolution of 0.5° × 0.5°, were derived from the Climate Research Unit (CRU) at http://www.cru.uea.ac.uk. The monthly mean geopotential height and wind vectors used for atmospheric circulation analysis and APVI calculation at 2.5° × 2.5° were obtained from NCEP/NCAR at https://psl.noaa.gov/data/reanalysis/reanalysis.shtml.

2.2 Terrestrial productivity data

The NDVI data were extracted from the Global Inventory Monitoring and Modeling Studies (GIMMS) with a spatial resolution of 1 × 1 km from 1982 to 2015 at https://ecocast.arc.nasa.gov/data/pub/gimms/3g.v1. The pixels with NDVI values greater and equal to 0.1 were treated as vegetated areas, and the pixels with NDVI values less than 0.1 were excluded. In this study, spring NDVI is the aggregated monthly mean NDVI of March, April, and May, and the yearly NDVI is the aggregated monthly mean NDVI in a year.

To study the mechanism of the anomalous APV-induced vegetation productivity effects, the observed GPP variations from eight flux towers, which represent eight eco-regions in China, were used. The observed GPP values were obtained from ChinaFLUX networks at http://www.chinaflux.org/. The detailed methods for GPP calculation were described by Yu et al. (2006, 2008, 2014). The eight eco-regions with their representative flux sites and vegetation, as well as the climatic drivers of GPP and NDVI, are listed in Table 1. The observed data periods for DXG and NMG are from 2004 to 2010, and those for other sites are from 2003 to 2010.

2.3 APVI calculation

We used a climate index, APVI, to represent the intensity of the spring APV. The method for APVI calculation is similar to that of Sui et al. (2014) and Li et al. (2017). First, a spring (average of March to May) southern boundary characteristic contour, H_0, was established based on the monthly 500-hPa geopotential height in the Northern Hemisphere from 1982 to 2015. The APVI is then calculated as

$$APVI = \rho R^2 \, \Delta\varphi\Delta\lambda\sum\sum\left(\mathrm{H}_0 - \mathrm{H}_{ij}\right)\cos\varphi_i \qquad (1)$$

where φ_i is the latitude where H_0 intersects the longitude, R is the radius of the Earth (6371 km), ρR^2 is 0.1, $\Delta\varphi = \Delta\lambda = \pi/72$, and H_{ij} is the 500-hPa geopotential height averaged over March to May in the northern area of H_0.

To detect the anomalous APVI years, a standard detrended APVI was first created by removing the linear trend and standardizing (by dividing by its standard deviation) the APVI time series. The thresholds of 1 and −1 were then used to divide the positive and negative APVI years. Positive APVI years are identified as those with APVI values greater than the

Table 1 The main characteristics of the flux towers and the climatic drivers of GPP and NDVI in the eight eco-regions

Eco-region	Site name	Latitude	Longitude	Vegetation	Climatic drivers of GPP	Climatic drivers of NDVI
NE	CBF	42°24′N	128°06′E	Forest	MT, MP, MS	MT, MS
NC	YCA	36°58′N	116°38′E	Crops	MT, MS	MT
SW	BNF	21°54′N	101°16′E	Forest	MT	MT
CC	QYF	26°44′N	115°03′E	Forest	MT, MS	MT
IM	NMG	44°08′N	116°18′E	Grassland	MP	MP
NW	HBG	37°40′N	101°20′E	Grassland	MP	MP
SC	DHF	23°09′N	112°30′E	Forest	MT, MS	MT
TP	DXG	30°29′N	91°03′E	Grassland	MP	-

Note: China's domains are divided into eight eco-regions of NE, IM, NW, NC, CC, SC, TP, and SW, representing Northeast China, Inner Mongolia, Northwest China, North China, Central China, Southeast China, Tibetan Plateau, and Southwest China, respectively. MT, MP, and MS represent monthly mean air temperature, monthly precipitation, and monthly mean solar radiation, respectively.

threshold of 1, while negative APVI years are those with APVI values less than the threshold of −1.

2.4 Statistical methods

2.4.1 Composite analysis

Composite analysis can effectively characterize climatic conditions for particular cases and has been widely used in climate research (Rudeva and Gulev 2011). To examine anomalous APV impacts on circulation and vegetation growth, composite analysis was applied to the average geopotential height, wind, air temperature, precipitation, and NDVI anomalies for the positive and negative APVI phase years.

2.4.2 Correlation analysis

Correlation analysis was used to detect the relationships between monthly GPP and climate factors and to examine the lagged vegetation productivity response to APV anomalies. The seasonal cycle of the observed monthly GPP and monthly climate factors were removed from the time series, and Student's t test was used to determine the statistical significance in the correlation analysis.

3 Results

3.1 Trends and variations in APVI

The APVI shows a significant decreasing trend from 1982 to 2015 ($P < 0.01$), which is consistent with Arctic warming (Fig. 1a). The positive APVI years were 1985, 1986, 1992, 1994, 2011, and 2015, and the negative APVI years were 1983, 1995, 1996, 2005, 2006, 2008, 2010, and 2013 (Fig. 1b).

3.2 Impacts of anomalous APV on atmospheric circulation

For the atmospheric circulation at 500 hPa, there is a marked difference between the positive and negative APVI phases near the Urals (45°N, 60°E), where negative and positive geopotential height anomalies dominated during the positive and negative APVI phases, respectively (Fig. 2a, b). This implies that the Ural blocking high-pressure system was weakened and enhanced during the positive and negative APVI phases, respectively. The Ural blocking high is one of the most important climate systems influencing China's weather pattern. Generally, a strong Ural blocking high inhibits air mass exchange between the Arctic and China's domain, but a weaker Ural blocking high enhances this exchange. Therefore, the atmospheric circulation at 500 hPa in the positive APVI phase is more conducive to southward cold air movement than that in the negative APVI phase.

The circulation patterns at 1000 hPa were consistent with those at 500 hPa. Northerly winds were enhanced, and positive geopotential height anomalies dominated most areas of China during the positive APVI phase. During the negative APVI phase, northerly winds were only enhanced in northern and northeastern China, while negative geopotential height anomalies dominated most areas of China (Fig. 2c, d). The anomalous atmospheric circulation patterns may have a great influence on the surface climate factors in China.

3.3 Impacts of anomalous APV on climate factors

The spatial patterns of temperature, precipitation, and solar radiation anomalies were consistent with the corresponding circulation patterns for the positive and negative APVI phases. During the positive APVI phase, the northerly winds were enhanced in most areas of China at 1000 hPa (Fig. 2c). The

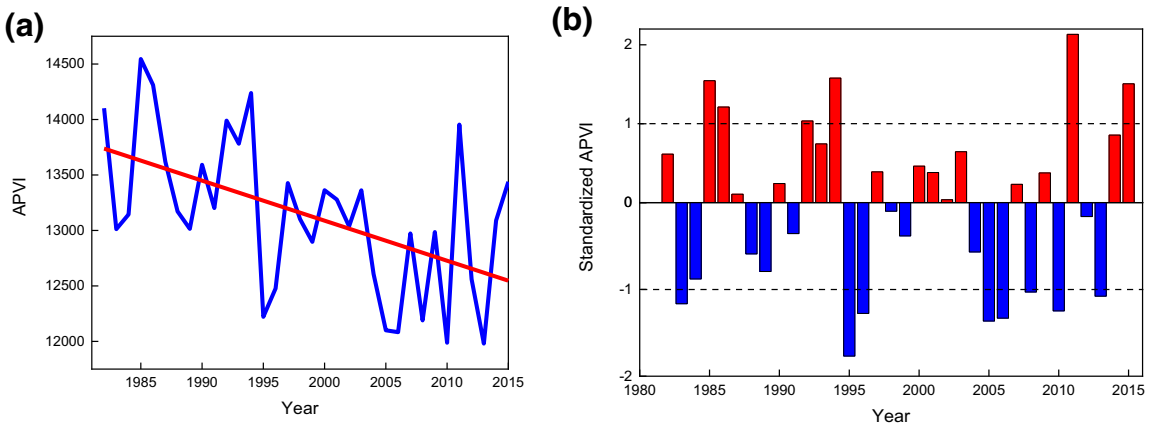

Fig.1 **a** Time series of APVI (blue) and its trends (red) and **b** the standardized APVI series. The thresholds of −1 and 1 are used to identify anomalous AVPI years

strengthening northerly winds sent large cold Arctic air masses towards China's domain, which decreased the air temperature by 0.2–0.5 °C in most eco-regions of China, including Inner Mongolia (IM), North China (NC), Central China (CC), Northwest China (NW), Southwest China (SW), and Southeast China (SC) (Fig. 3a). Meanwhile, as positive geopotential height anomalies dominated most parts of China, the high pressure and downdrafts were enhanced, reducing cloud and precipitation formation. Therefore, negative precipitation and positive solar radiation anomalies dominated most areas of China (Fig. 3c, e), and the precipitation reductions ranged from 15 to 30% in NE and NW and, generally, from 5 to 15% in the other regions.

During the negative APVI phase, the northerly winds were weakened in most eco-regions of China and were only enhanced in NE and IM. Therefore, the air temperature anomalies were between −0.2 and −0.5 °C in NE and IM and between 0.2 and 0.5 °C in other eco-regions of China (Fig. 3b). Since a cyclone system existed near northeastern China at 500 hPa (Fig. 2b), which was conducive to forming precipitation, the precipitation anomalies in NE ranged from 15 to 30% (Fig. 3d). Additionally, the warm and humid air from the Indian and Pacific Oceans met the northern cold air in southern China (Fig. 2d), which formed precipitation in most areas of NW, TP, CC, SC, and SW, with precipitation anomalies of 5–30%. As negative geopotential height anomalies dominated most regions of China, the updrafts were enhanced, which was conducive to forming clouds. Therefore, negative solar radiation anomalies occurred in most areas of China (Fig. 3f).

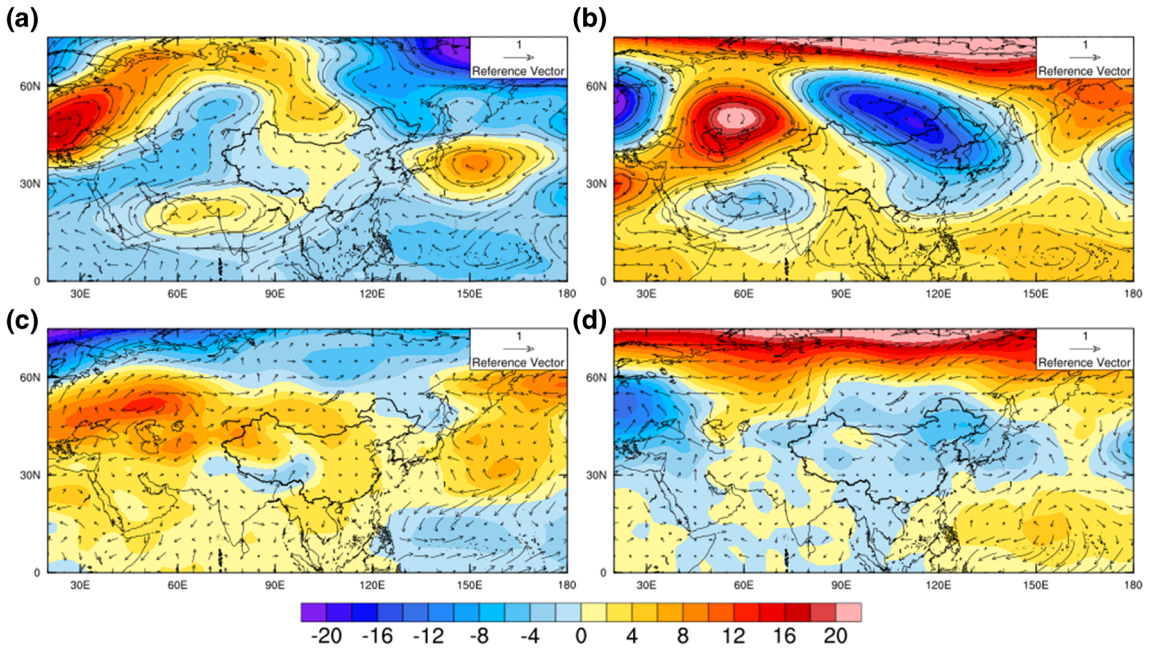

Fig. 2 Composite geopotential height (gpm) and wind anomalies (10 m/s) for APVI phases. **a** Positive APVI phase at 500 hPa; **b** negative APVI phases at 500 hPa; **c** positive APVI phase at 1000 hPa, and **d** negative APVI phases at 1000 hPa

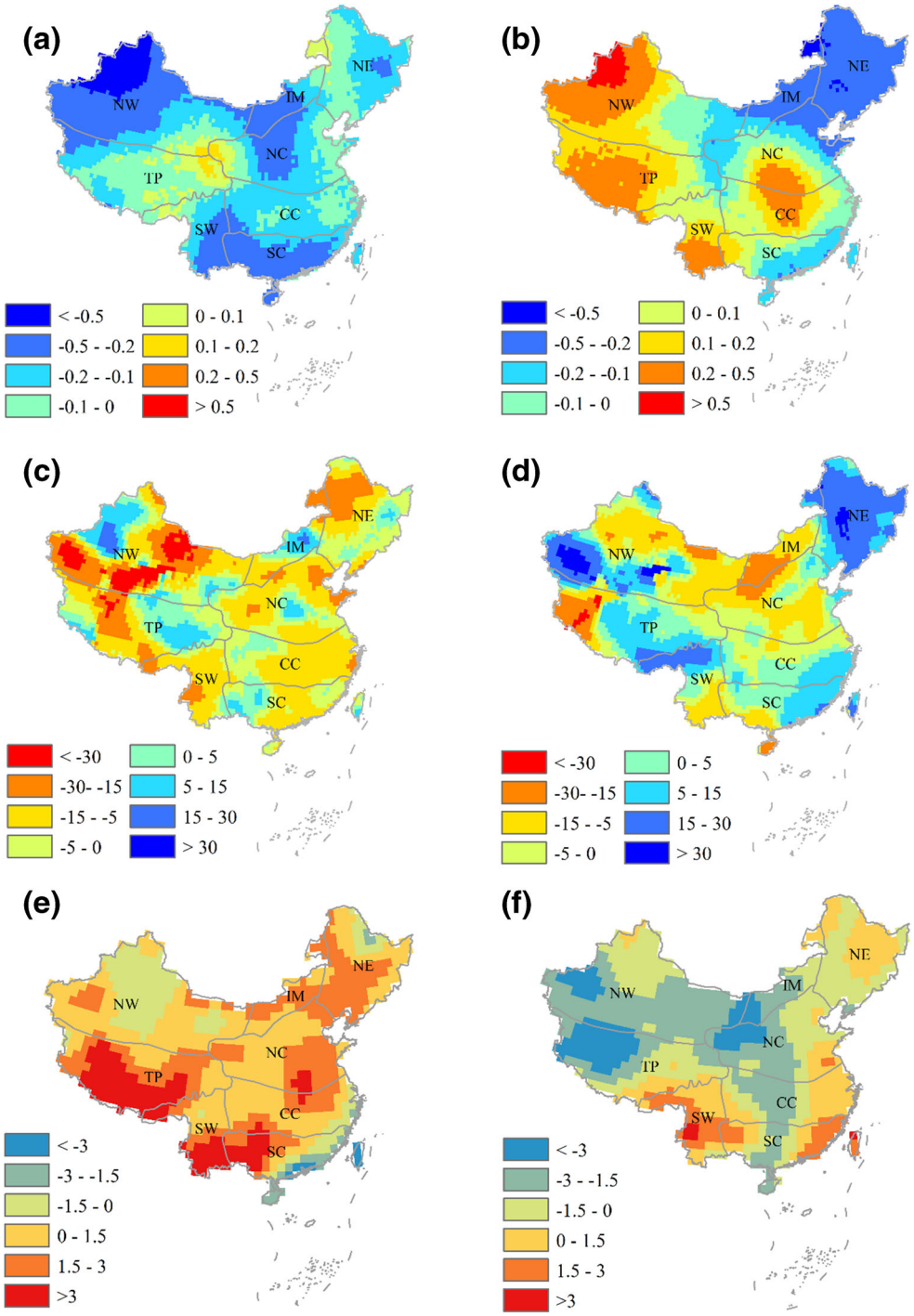

Fig. 3 Composite of spring (March to May) mean temperature (°C), total precipitation (%), and mean solar radiation (W/m^2) anomalies for the positive and negative APVI phases. **a** Temperature in the positive phase; **b** temperature in the negative phase; **c** precipitation in the positive phase; **d** precipitation in the negative phase; **e** solar radiation in the positive phase, and **f** solar radiation in the negative phase. China's domains are divided into eight eco-regions of NE, IM, NW, NC, CC, SC, TP, and SW, representing Northeast China, Inner Mongolia, Northwest China, North China, Central China, Southeast China, Tibetan Plateau, and Southwest China, respectively

3.4 Impacts of anomalous APV conditions on spring vegetation activity

The anomalous climate factors during the positive and negative APVI phases were expected to affect China's vegetation activity in the spring. In the positive APVI phase, positive and negative NDVI anomalies occupied 51.4 and 48.6% of China's vegetated areas, respectively. Negative vegetation activity mainly occurred in SW and TP, with the lowest NDVI anomalies less than −10%, while positive vegetation activity mainly occurred in the other eco-regions, with the highest NDVI anomalies greater than 10% (Fig. 4a). In the negative APVI phase, positive and negative NDVI anomalies occupied 46.8 and 53.2% of China's vegetated areas, respectively. Negative vegetation activity mainly occurred in NE and IM, with NDVI anomalies between −5 and −10%, while positive vegetation activity occurred in the other eco-regions, with NDVI anomalies between 5 and 10%.

3.5 Lagged vegetation productivity response to anomalous APV

The lagged vegetation productivity responses are different between the positive and negative APVI phases. For the yearly NDVI, 55% of China's vegetated area was covered by negative anomalies during the positive APVI phase, but 65% of China's vegetated area was covered by positive yearly NDVI anomalies during the negative APVI phase. The negative NDVI anomalies mainly occurred in NE, IM, NC, SW, and TP during the positive APVI phase, with values mostly between −1 and −5% (Fig. 5a). Positive NDVI anomalies were widely distributed in NE, NC, CC, SC, SW, and NW during the negative APVI phase, with most of the values between 1 and 10% (Fig. 5b).

Comparison of the difference between yearly and spring NDVI anomalies revealed that more negative lagged vegetation productivity responses occurred in the positive phase than in the negative APVI phase. During the positive and negative APVI phases, negative lagged vegetation productivity responses occurred in 54.5 and 32.8% of China's vegetated areas, respectively, and positive lagged vegetation productivity responses occurred in 45.5 and 67.2% of China's vegetated areas, respectively (Fig. 5c, d).

4 Discussion

4.1 Spring vegetation activity in China linked to APV anomalies

Understanding the factors controlling vegetation productivity is an effective way to explain the impacts of APV anomalies on NDVI. We first explored the observed relationship between GPP and climate factors at ChinaFLUX sites to determine the climatic drivers of GPP at the site scale, and then we combined the relationships at the site scale with large-scale distributions of the climate factors and NDVI to evaluate the climatic drivers of NDVI and to explain the links between spring NDVI variability and APV anomalies in China.

As shown in Fig. 6, positive correlations between air temperature and GPP are observed at CBF ($R^2 = 0.72$, $P < 0.001$), BNF ($R^2 = 0.57$, $P < 0.001$), QYF ($R^2 = 0.91$, $P < 0.001$), DHF ($R^2 = 0.73$, $P < 0.001$), and YCA ($R^2 = 0.67$, $P < 0.001$), and positive correlations between solar radiation and GPP are observed at CBF ($R^2 = 0.63$, $P < 0.001$), QYF ($R^2 = 0.77$, $P < 0.001$), DHF ($R^2 = 0.66$, $P < 0.001$), and YCA ($R^2 = 0.72$, $P < 0.001$). Precipitation is positively correlated with GPP in CBF ($R^2 = 0.42$, $P < 0.01$), NMG ($R^2 = 0.88$, $P < 0.001$), HBG ($R^2 = 0.41$, $P < 0.01$), and DXG ($R^2 = 0.58$, $P < 0.01$).

The spatial patterns of NDVI anomalies in each eco-region in the positive and negative APVI phases can be explained using the observed GPP-climate relationships at the corresponding ChinaFLUX site. Air temperature is positively correlated with GPP in SW, CC, SC, and NC. Negative and positive air temperature anomalies dominated most areas in SW, CC, SC, and NC during the positive and negative APVI phases, respectively (Fig. 3a, b). Therefore, negative and positive NDVI anomalies occurred in most areas of SW, CC, SC, and NC during the positive and negative APVI phases, respectively (Fig. 4). Precipitation is positively correlated with GPP in NW and IM. Positive and negative precipitation anomalies dominated most vegetated areas in NW and IM during the positive and negative APVI phases, respectively (Fig. 3c, d). Therefore, positive and negative NDVI anomalies occurred in most areas in NW and IM during the positive and negative APVI phases, respectively (Fig. 4). Both air temperature and solar radiation are positively correlated with GPP in NE.

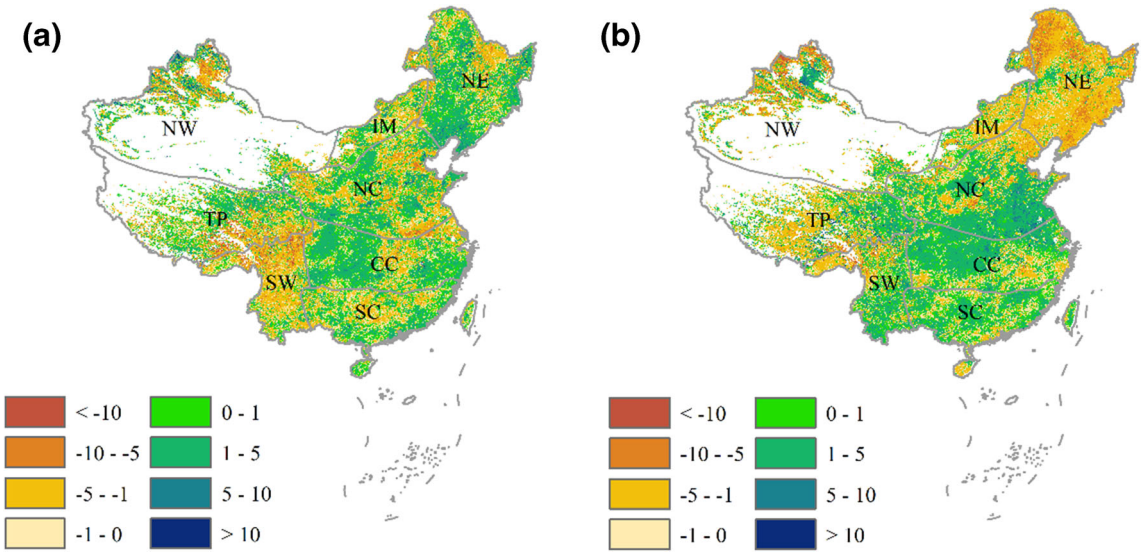

Fig. 4 Spatial pattern of composite spring NDVI anomaly (%) for **a** positive and **b** negative APVI phases

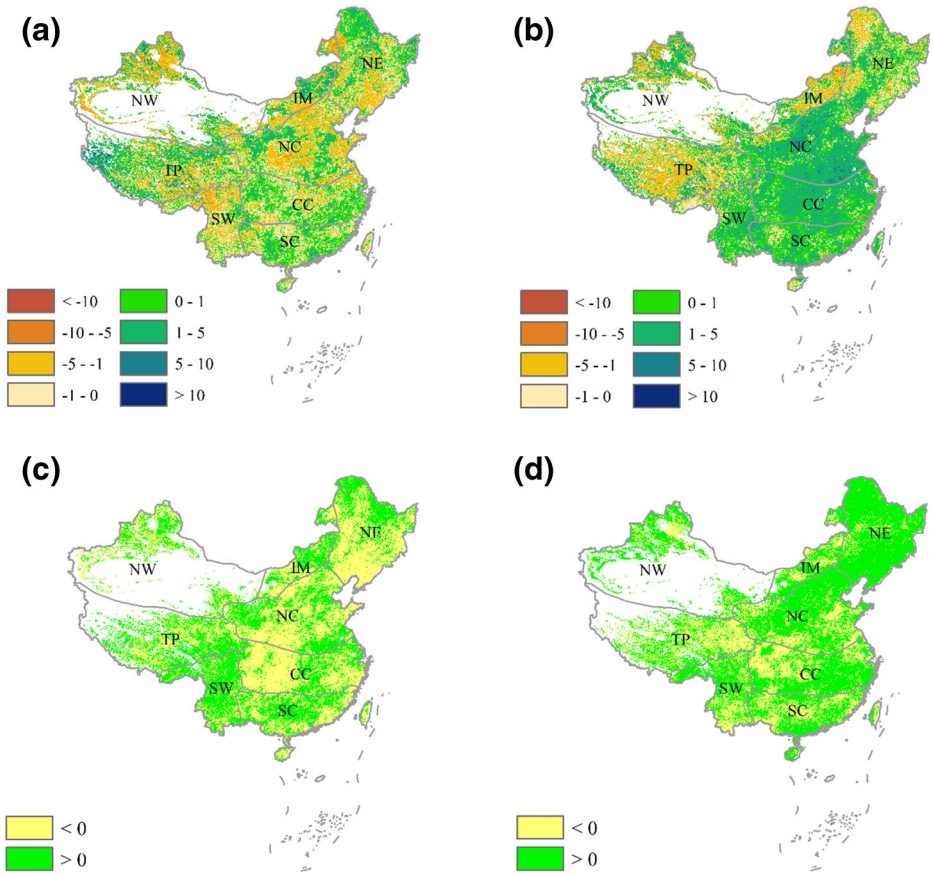

Fig. 5 Spatial pattern of composite yearly NDVI anomalies (%) for the **a** positive and **b** negative APVI phases; spatial pattern of difference between yearly and spring NDVI anomalies for the **c** positive APVI phase and **d** negative APVI phase. Positive and negative values in **c** and **d** indicate positive and negative lagged effects on productivity, respectively

Positive NDVI anomalies occurred in NE in the positive APVI phase and were attributed to positive air temperature and solar radiation anomalies, while negative NDVI anomalies occurred in NE in the negative APVI phase and were attributed to negative air temperature and solar radiation anomalies.

The TP is the highest plateau in the world. The start date of the growing season at DXG is far later than that of other sites because of its high elevation (4333 m). Since the monthly GPP in March is zero at DXG, we have to use the data from April to June to explore the vegetation–climate relationships. In DXG, GPP is positively correlated with precipitation. However, the spatial pattern of NDVI anomalies cannot be fully explained by the pattern of precipitation anomalies in the TP. This discrepancy might be attributed to the delayed phonological phase, spatial heterogeneities (Cong et al. 2017), and elevation-related precipitation differences in the TP (Zheng et al. 2020).

Although NDVI is not a GPP measurement, NDVI can be a proxy for the primary productivity of the terrestrial biosphere (Myneni et al. 1997). Therefore, the responses of NDVI and GPP to climate factors should have similar characteristics. However, by comparing the spatial pattern of NDVI with the climate drivers, it is found that the number of climatic drivers for GPP is greater than that for NDVI (Table 1). For example, at YCA, QYF, and DHF, the climatic drivers of GPP are air temperature and solar radiation, but that of NDVI is only temperature. One possible reason of this discrepancy is the influence of human activity. The change of NDVI is caused by both climate and human factors, but the change of the observed GPP is only affected by climate factor. Human activities, such as land use change, fertilization, and irrigation will lead to the change of NDVI (Mueller et al. 2014). Another possible reason is the spatial heterogeneity of NDVI. In this study, the change of NDVI value in a pixel reflects the change of vegetation greenness within 1 km^2, which may contain more than one kind of ecosystem. Therefore, GPP is more sensitive to climate change than NDVI.

4.2 Comparison of the impacts of positive and negative APVI phases

Although the APV-induced spatial distributions of the spring NDVI anomalies were different between the positive and negative APVI phases, both APVI phases caused almost 50% of the positive and negative spring NDVI anomalies in China. Positive and negative spring NDVI anomalies occupied 51.4 and 48.6% of China's vegetated areas during the positive APVI phase, while positive and negative spring NDVI

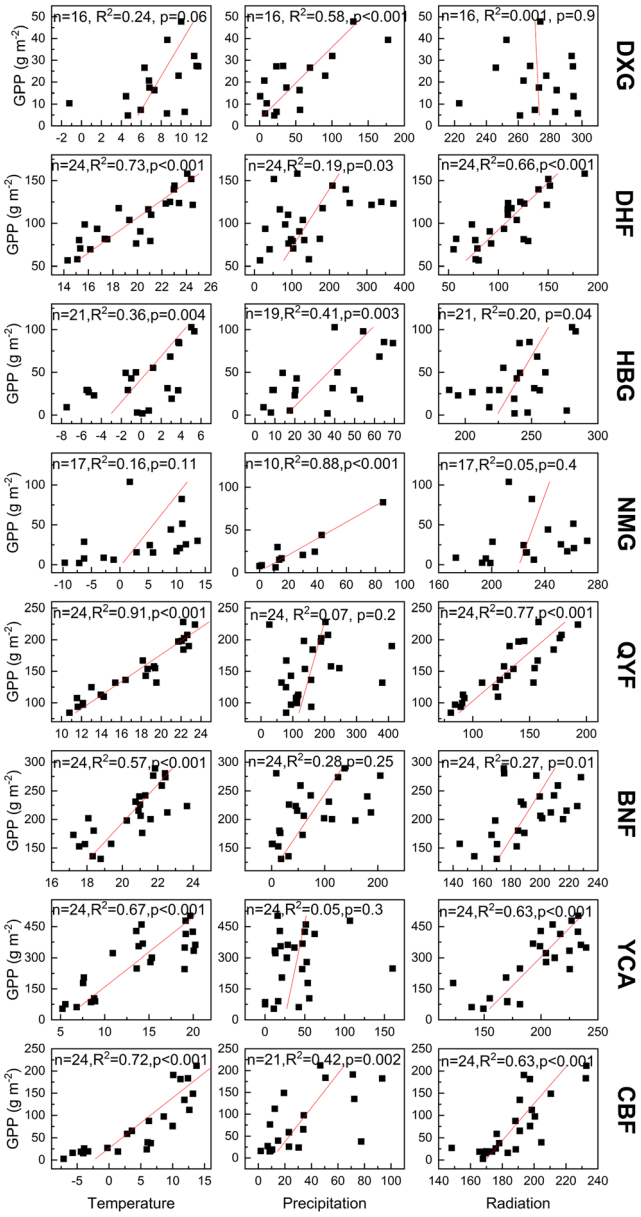

Fig. 6 Relationships between monthly GPP and monthly mean temperature (°C), monthly precipitation (mm), and monthly mean solar radiation (W/m^2) at the ChinaFLUX sites DXG, DHF, HBG, NMG, QYF, BNF, YCA, and CBF. Here, the monthly GPP data include data from April to June for DXG and from March to May for the other seven sites

anomalies occupied 46.8 and 53.2% of China's vegetated areas during the negative APVI phase. In terms of the eco-regional mean, the number of eco-regions with positive and negative NDVI anomalies is four for both positive and negative APVI phases. Vegetation activity declined in NC, IM, TP, and SW during the positive APVI phase and declined in NE, IM, NW, and TP during the negative APVI phase. Vegetation activity increased in NE, SC, NW, and CC during the positive APVI phase and increased in NC, SC, SW, and CC during the negative APVI phase (Table 2).

For the positive APVI phase, vegetation productivity exhibited adverse lagged effects in NE, NC, NW, and CC, where the eco-regional NDVI anomalies were 0.65%, −0.07%, 0.01%, and 0.46% in spring and decreased to −0.06%, −0.53%, −0.50%, and −0.10% for the full year, respectively. However, vegetation growth exhibited beneficial lagged effects in SC, IM, TP, and SW, where the NDVI anomalies were 0.01%, −0.57%, −0.68%, and −1.93% in spring, and each increased to 0.02%, −0.26%, 0.55%, and −0.75%, respectively (Table 2).

For the negative APVI phase, most of the negative vegetation activity in the spring could be compensated by climate conditions in the subsequent summer and autumn, and beneficial lagged effects occurred in almost all of China's region except for TP. The spring NDVI anomalies were −2.69%, 0.81%, 0.64%, −1.2%, −1.54%, 0.10%, and 1.0% in NE, NC, SC, IM, NW, SW, and CC, respectively, and each was lower than the yearly NDVI anomalies of 0.07%, 1.91%, 0.98%, −0.39%, 0.24%, 0.70%, and 1.51% in the corresponding eco-regions.

The eco-region IM, located in the arid and semiarid area of China and mainly covered by grassland, is the only eco-region with negative spring and yearly NDVI values in both positive and negative APVI phases. Previous studies have demonstrated that vegetation in IM is most vulnerable to climate change (Zhang et al. 2011; John et al. 2013; Bao et al. 2014), and our research suggests that vegetation in IM is most vulnerable to APV anomalies.

4.3 Lagged vegetation productivity responses linked to APV anomalies

By comparing the lagged vegetation productivity responses between the positive and negative APVI phases, 67.2% of China's vegetated areas exhibited positive lagged responses during the negative APVI phase, but only 45.5% of China's vegetated areas exhibited positive lagged effects during the

Table 2 Eco-regional mean spring and year NDVI anomalies for the positive and negative APVI phases

Eco-region	Positive APVI phase		Negative APVI phase	
	Yearly (%)	Spring (%)	Yearly (%)	Spring (%)
NE	−0.06	0.65	0.07	−2.69
NC	−0.53	−0.07	1.91	0.81
SC	0.02	0.01	0.98	0.64
IM	−0.26	−0.57	−0.39	−1.20
NW	−0.50	0.01	0.24	−1.54
TP	0.55	−0.68	−0.39	−0.14
SW	−0.75	−1.93	0.70	0.10
CC	−0.10	0.46	1.51	1.00

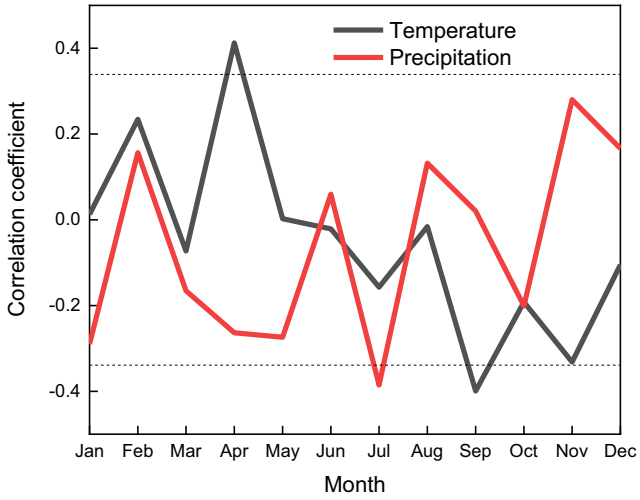

Fig. 7 Correlation coefficients between detrended APVI and detrended monthly mean air temperature and monthly precipitation averaged over China. Dashed lines indicate the thresholds of the 95% significance level

positive APVI phase. This difference may be attributed to climate conditions in the subsequent summer and autumn. The association between APVI and climate conditions in the subsequent summer and autumn is understandable because APV-induced spring climate change alters the ecosystem productivity and the seasonality of important ecosystem feedbacks to the atmosphere and climate system, which results in changes in temperature and precipitation in the following months.

We then examine the relationships between the detrended APVI and detrended monthly air temperature and precipitation averaged over China. The APVI is significantly correlated with air temperature in April, which is consistent with our previous results of spring NDVI variability. Additionally, we found significant correlations between APVI and precipitation in July and air temperature in September (Fig. 7). Hence, we further examine the spatial distributions of the correlation coefficients.

Spatially, monthly precipitation in July was negatively associated with the APVI in NC, NW, and parts of TP and positively associated with the APVI in most areas of NE, CC, SC, SW, and TP (Fig. 8a). Furthermore, the monthly mean air temperature of September was negatively correlated with the APVI in NE, IM, NW, NC, SW, and CC and positively associated with the APVI in TP (Fig. 8b).

As the positive (negative) APVI phase corresponds to higher (lower) detrended APVI values, when the correlation coefficients between the APVI and climate factors are positive (negative), then the positive APVI phase corresponds to higher (lower) climate factor values, and the negative APVI phase corresponds to lower (higher) climate factor values. The lagged vegetation productivity responses for the anomalous APVI phases could be interpreted by combining the spatial distribution of the correlation coefficients with the climate drivers of NDVI in each eco-region.

As displayed in Table 1, NDVI variability in NE, NC, CC, SC, and SW was controlled by temperature variation, while that in IM, NW, and TP was controlled by precipitation variation. During the positive APVI phase, adverse lagged responses occurred in NE, NC, NW, and CC, while beneficial lagged responses occurred in SC, IM, TP, and SW. The adverse lagged responses in NE, NC, and CC were attributed to the negative correlation between the APVI and temperature in September, which caused lower temperatures in the positive APVI phase and resulted in a decrease in the NDVI in the autumn. The adverse lagged effects in NW were attributed to the negative APVI–precipitation relationship in July, which caused lower precipitation in the positive APVI phase and resulted in the decreased NDVI in NW. Furthermore, the beneficial lagged responses that occurred in SC and SW were attributed to a

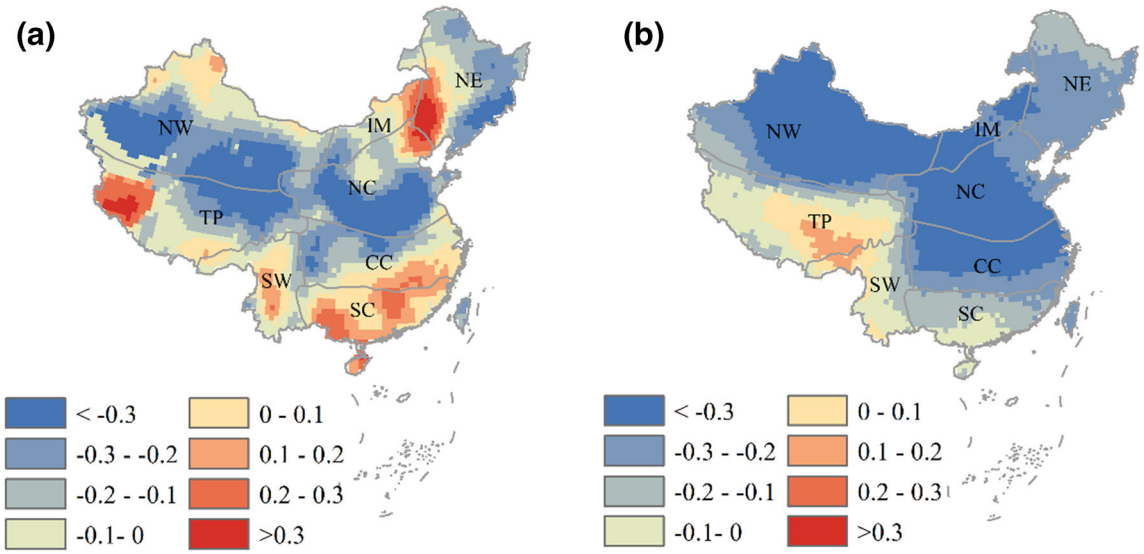

Fig. 8 Spatial pattern of correlation coefficients between the detrended APVI and detrended **a** precipitation in July and **b** temperature in September

positive APVI–temperature relationship, which caused higher temperatures in September and resulted in NDVI increases in SC and SW. The beneficial lagged responses that occurred in IM and TP were attributed to positive APVI– precipitation relationships, which caused higher precipitation in July and resulted in NDVI increases in IM and TP.

During the negative APVI phase, beneficial lagged responses occurred in almost all of China's region except for TP. The beneficial lagged responses that occurred in NE, NC, CC, SC, and SW were attributed to negative APVI–temperature relationships in September, which caused higher temperatures and resulted in an increased NDVI. The beneficial lagged responses that occurred in IM and NW were attributed to negative APVI–precipitation relationships, which caused higher precipitation in July and resulted in NDVI increases in IM and NW. The adverse lagged responses that occurred in the TP may be attributed to positive APVI–temperature relationships in September, which caused lower temperatures in the negative APVI phase and resulted in a decreased NDVI. However, the observations of GPP at the site scale did not show significant relationships with temperature. The climate drivers of NDVI in TP need further research.

Buermann et al. (2018) reported that there were contrasting lagged productivity responses to spring warmth across northern ecosystems. In this study, we found that diverse lagged productivity responses were associated with circulation patterns in the early stages, which supplements the findings of Buermann et al.

5 Conclusions

In this paper, we examined the impacts of APV anomalies on spring vegetation variability and lagged vegetation productivity responses in China and discussed the linkage between APV anomalies and vegetation variability. We found that both strong and weak APV have almost equal negative impacts on spring vegetation growth in China, e.g., negative NDVI anomalies occurred in 48.6 and 53.2% of China's vegetated areas during the positive and negative APVI phases, respectively. However, a large difference exists in the lagged vegetation productivity responses between the positive and negative APVI phases. The areal percentage of adverse lagged productivity responses is 54.5% in the positive APVI phase, which is much higher than that of 32.8% in the negative APVI phase. The areal percentage of beneficial lagged productivity responses is 45.5% in the positive APVI phase, which is much lower than that of 67.2% in the negative APVI phase. Under a strong APV, adverse lagged responses occurred in NE, NC, NW, and CC, and beneficial lagged effects occurred in SC, IM, TP, and SW. Under a weak APV, adverse lagged responses occurred only in TP, and beneficial lagged effects occurred in other parts of China.

An APV anomaly corresponds to an anomalous atmospheric circulation pattern, which is the main cause of anomalous spring air temperature, precipitation, and solar radiation changes in China, and changes in these climate factors are the main drivers of NDVI variability. Anomalous air temperature change is the main reason for NDVI variability in SC, CC, NC, and SC, and anomalous precipitation change is a driver of the changes in NDVI in NW and IM. Both anomalous air temperature and solar radiation changes are the main drivers of NDVI variability in NE.

The lagged vegetation productivity responses were mainly attributed to the strong association between the APVI and precipitation in July and temperature in September. The lower precipitation and lower temperature occurring in the subsequent July and September were the main reasons for the adverse lagged vegetation productivity responses in the positive APVI phase. In contrast, the higher precipitation and higher temperature occurring in the subsequent July and September were the reasons for the beneficial lagged vegetation productivity responses in the negative APVI phase. The strong association between spring APV anomalies and yearly NDVI variability makes the APVI useful in vegetation productivity prediction.

The present study used the intensity of the APV to represent the variation in the APV and did not consider other indices, such as the area or position of the APV. In future studies, we need to include more indices to more accurately predict the impacts of APV anomalies on vegetation variability in China.

Acknowledgements We would like to thank the editor and reviewers for their valuable comments and suggestions. We thank the scientific teams for Climatic Research Unit (University of East Anglia) and NCAS, NASA, the NCEP/NCAR Reanalysis Project, and the ChinaFLUX. We would like to thank these agencies for providing the data for our work.

Author contribution He Gong performed the data analyses and wrote the manuscript. Mei Huang contributed to the conception of the study and modified the manuscript. Zhaosheng Wang collected the data. Shaoqiang Wang gave some suggestions for modification. Fengxue Gu helped perform the analysis with constructive discussions.

Funding This study is supported by the Science and Technology Basic Resources Investigation Program of China (2017FY101301), the National Key Research and Development Program of China (2017YFC0503905), and the Chinese National Natural Science Fund (41971135).

Availability of data and materials The NDVI data were obtained from the Global Inventory Monitoring and Modeling Studies (GIMMS) (https://ecocast.arc.nasa.gov/data/pub/gimms/3g.v1). The monthly mean precipitation (mm) and surface air temperature (°C) were obtained from the Climate Research Unit (CRU) (http://www.cru.uea.ac.uk). The monthly mean geopotential height (gpm), wind speed (m/s), and solar radiation (W/m^2) were downloaded from NCEP/NCAR Reanalysis Project at the NOAA/ESRL Physical Sciences Laboratory (https://psl.noaa.gov/data/reanalysis/reanalysis.shtml). The observed GPP values (g/m^2) were obtained from ChinaFLUX (http://www.chinaflux.org/).

Code availability Not applicable.

Declarations

Ethics approval and consent to participate Not applicable. Our research did not involve human participants.

Consent for publication Not applicable.

Conflict of interest statement The authors declare no competing interests.

References

Angell JK, Korshover J (1977) Variation in size and location of the 300 mb north circumpolar vortex between 1963 and 1975. Mon Weather Rev 105(1):19–25

Bao G, Qin Z, Bao Y, Zhou Y, Li W, Sanjjav A (2014) NDVI-based long-term vegetation dynamics and is response to climatic change in the Mongolian Plateau. Remote Sens 6(9):8337–8358. https://doi.org/10.3390/rs6098337

Bhatt US, Walker DA, Raynolds MK, Comiso JC, Epstein HE, Jia G, Gens R, Pinzon JE, Tucker CJ, Tweedie CE, Webber PJ (2010) Circumpolar arctic tundra vegetation change is linked to sea ice decline. Earth Interact 14. https://doi.org/10.1175/2010ei315.1

Buermann W, Forkel M, O'Sullivan M, Sitch S, Friedlingstein P, Haverd V et al (2018) Widespread seasonal compensation effects of spring warming on northern plant productivity. Nature 562(7725):110–115. https://doi.org/10.1038/s41586-018-0555-7

Bunn AG, Goetz SJ, Kimball JS, Zhang K (2007) Northern high-latitude ecosystems respond to climate change. Eos Trans AGU 88(34):333–335. https://doi.org/10.1029/2007eo340001

Cohen J, Screen JA, Furtado JC, Barlow M, Whittleston D, Coumou D, Francis J, Dethloff K, Entekhabi D, Overland J, Jones J (2014) Recent Arctic amplification and extreme mid-latitude weather. Nat Geosci 7(9):627–637. https://doi.org/10.1038/ngeo2234

Cohen J, Zhang X, Francis J, Jung T, Kwok R, Overland J, Ballinger TJ, Bhatt US, Chen HW, Coumou D, Feldstein S, Gu H, Handorf D, Henderson G, Ionita M, Kretschmer M, Laliberte F, Lee S, Linderholm HW, Maslowski W, Peings Y, Pfeiffer K, Rigor I, Semmler T, Stroeve J, Taylor PC, Vavrus S, Vihma T, Wang S, Wendisch M, Wu Y, Yoon J (2020) Divergent consensuses on Arctic amplification influence on midlatitude severe winter weather. Nat Clim Chang 10(1):20–25. https://doi.org/10.1038/s41558-019-0662-y

Cong N, Shen M, Yang W, Yang Z, Zhang G, Piao S (2017) Varying responses of vegetation activity to climate changes on the Tibetan Plateau grassland. Int J Biometeorol 61(8):1433–1444. https://doi.org/10.1007/s00484-017-1321-5

Francis J, Skific N (2015) Evidence linking rapid Arctic warming to mid-latitude weather patterns. Philos Trans R Soc A Math Phys Eng Sci 373(2045):20140170. https://doi.org/10.1098/rsta.2014.0170

Francis J, Vavrus S (2012) Evidence linking Arctic amplification to extreme weather in mid-latitudes. Geophys Res Lett 39. https://doi.org/10.1029/2012gl051000

Frauenfeld OW, Davis RE (2000) The influence of El Nino-Southern Oscillation events on the northern hemisphere 500 hPa circumpolar vortex. Geophys Res Lett 27(4):537–540

Hufkens K, Friedl MA, Keenan TF, Sonnentag O, Bailey A, O'Keefe J, Richardson AD (2012) Ecological impacts of a widespread frost event following early spring leaf-out. Glob Chang Biol 18(7):2365–2377. https://doi.org/10.1111/j.1365-2486.2012.02712.x

Inouye DW (2008) Effects of climate change on phenology, frost damage, and floral abundance of montane wildflowers. Ecology 89(2):353–362. https://doi.org/10.1890/06-2128.1

John R, Chen J, Ou-Yang Z-T, Xiao J, Becker R, Samanta A, Ganguly S, Yuan W, Batkhishig O (2013) Vegetation response to extreme climate events on the Mongolian Plateau from 2000 to 2010. Environ Res Lett 8(3). https://doi.org/10.1088/1748-9326/8/3/035033

Kim B-M, Son S-W, Min S-K, Jeong J-H, Kim S-J, Zhang X, Shim T, Yoon JH (2014) Weakening of the stratospheric polar vortex by Arctic sea-ice loss. Nat Commun 5. https://doi.org/10.1038/ncomms5646

Li J, Fan K, Xu J, Powell AM Jr, Kogan F (2017) The effect of preceding wintertime Arctic polar vortex on springtime NDVI patterns in boreal Eurasia, 1982-2015. Clim Dyn 49(1-2):23–35. https://doi.org/10.1007/s00382-016-3324-z

Liu Z (1986) The calculation of polar vortex intensity in Northern Hemisphere and relationship with temperature in China. Meteorological Monthly 12(s1):84–89

Mitchell DM, Gray LJ, Anstey J, Baldwin MP, Charlton-Perez AJ (2013) The influence of stratospheric vortex displacements and splits on surface climate. J Clim 26(8):2668–2682. https://doi.org/10.1175/jcli-d-12-00030.1

Mueller T, Dressler G, Tucker CJ, Pinzon JE, Leimgruber P, Dubayah RO, Hurtt G, Böhning-Gaese K, Fagan W (2014) Human land-use practices lead to global long-term increases in photosynthetic capacity. Remote Sens 6(6):5717–5731. https://doi.org/10.3390/rs6065717

Myneni RB, Keeling CD, Tucker CJ, Asrar G, Nemani RR (1997) Increased plant growth in the northern high latitudes from 1981 to 1991. Nature 386(6626):698–702. https://doi.org/10.1038/386698a0

Noormets A, McNulty SG, DeForest JL, Sun G, Li Q, Chen J (2008) Drought during canopy development has lasting effect on annual carbon balance in a deciduous temperate forest. New Phytol 179(3):818–828. https://doi.org/10.1111/j.1469-8137.2008.02501.x

Norby RJ, Hartz-Rubin JS, Verbrugge MJ (2003) Phenological responses in maple to experimental atmospheric warming and CO2 enrichment. Glob Chang Biol 9(12):1792–1801. https://doi.org/10.1111/j.1365-2486.2003.00714.x

Overland JE, Wang M (2010) Large-scale atmospheric circulation changes are associated with the recent loss of Arctic sea ice. Tellus Ser A Dyn Meteorol Oceanogr 62(1):1–9. https://doi.org/10.1111/j.1600-0870.2009.00421.x

Overland JE, Francis JA, Hall R, Hanna E, Kim S-J, Vihma T (2015) The melting Arctic and midlatitude weather patterns: are they connected? J Clim 28(20):7917–7932. https://doi.org/10.1175/jcli-d-14-00822.1

Pearson RG, Phillips SJ, Loranty MM, Beck PSA, Damoulas T, Knight SJ, Goetz SJ (2013) Shifts in arctic vegetation and associated feedbacks under climate change. Nat Clim Chang 3(7):673–677. https://doi.org/10.1038/nclimate1858

Peng J, Dan L, Ying K, Yang S, Tang X, Yang F (2020) China's interannual variability of net primary production is dominated by the Central China region. J Geophys Res Atmos 125:e2020JD033362. https://doi.org/10.1029/2020JD033362

Pinzon JE, Tucker CJ (2014) A non-stationary 1981–2012 AVHRR NDVI3g time series. Remote Sens 6(8):6929–6960

Rudeva I, Gulev SK (2011) Composite analysis of North Atlantic extratropical cyclones in NCEP-NCAR reanalysis data. Mon Weather Rev 139(5):1419–1446. https://doi.org/10.1175/2010mwr3294.1

Screen JA, Simmonds I (2010) The central role of diminishing sea ice in recent Arctic temperature amplification. Nature 464(7293):1334–1337. https://doi.org/10.1038/nature09051

Screen JA, Simmonds I (2013) Exploring links between Arctic amplification and mid-latitude weather. Geophys Res Lett 40(5):959–964. https://doi.org/10.1002/grl.50174

Serreze MC, Barry RG (2011) Processes and impacts of Arctic amplification: a research synthesis. Glob Planet Chang 77(1-2):85–96. https://doi.org/10.1016/j.gloplacha.2011.03.004

Serreze MC, Walsh JE, Chapin FS, Osterkamp T, Dyurgerov M, Romanovsky V et al (2000) Observational evidence of recent change in the northern high-latitude environment. Clim Chang 46(1-2):159–207. https://doi.org/10.1023/a:1005504031923

Shepherd TG (2016) Effects of a warming Arctic. Science 353(6303): 989–990. https://doi.org/10.1126/science.aag2349

Stroeve J, Holland MM, Meier W, Scambos T, Serreze M (2007) Arctic sea ice decline: faster than forecast. Geophys Res Lett 34(9). https://doi.org/10.1029/2007gl029703

Sturm M, Racine C, Tape K (2001) Increasing shrub abundance in the Arctic. Nature 411(6837):546–547. https://doi.org/10.1038/35079180

Sui C, Zhang Z, Cai Y, Wu H (2014) Using the physical decomposition method to study the effects of Arctic factors on wintertime temperatures in the Northern Hemisphere and China. Adv Polar Sci 4:213–221

Tape K, Sturm M, Racine C (2006) The evidence for shrub expansion in Northern Alaska and the Pan-Arctic. Glob Chang Biol 12(4):686–702. https://doi.org/10.1111/j.1365-2486.2006.01128.x

Thompson DWJ, Wallace JM (1998) The Arctic oscillation signature in the wintertime geopotential height and temperature fields. Geophys Res Lett 25(9):1297–1300. https://doi.org/10.1029/98gl00950

Thompson DWJ, Baldwin MP, Wallace JM (2002) Stratospheric connection to Northern Hemisphere wintertime weather: implications for prediction. J Clim 15(12):1421–1428

Tucker CJ, Slayback DA, Pinzon JE, Los SO, Myneni RB, Taylor MG (2001) Higher northern latitude normalized difference vegetation index and growing season trends from 1982 to 1999. Int J Biometeorol 45(4):184–190

Walsh JE (2014) Intensified warming of the Arctic: causes and impacts on middle latitudes. Glob Planet Chang 117:52–63. https://doi.org/10.1016/j.gloplacha.2014.03.003

Wang D, Liu C, Liu Y (2008) A preliminary analysis of features and causes of the snow storm event over the Southern China in January 2008. Acta Meteorol Sin 66(3):405–442

Wang SYS, Lin Y-H, Lee M-Y, Yoon J-H, Meyer JDD, Rasch PJ (2017) Accelerated increase in the Arctic tropospheric warming events surpassing stratospheric warming events during winter. Geophys Res Lett 44(8):3806–3815. https://doi.org/10.1002/2017gl073012

Xiong G, Chen Q, Wei L, Hu D (2012) Influences of the deflection of stratospheric polar vortex on winter precipitation of China. J Appl Meteor Sci 23(6):683–690

Yi M, Chen Y, Zhou R (2009) Analysis on isentropic potential vorticity for the snow calamity in South China and the stratospheric polar vortex in 2008. Plateau Meteorol 28(4):880–888

Yu G, Wen X, Sun X, Tanner BD, Lee X, Chen J (2006) Overview of ChinaFLUX and evaluation of its eddy covariance measurement. Agric For Meteorol 137(3-4):125–137. https://doi.org/10.1016/j.agrformet.2006.02.011

Yu G, Zhang L, Sun X, Fu Y, Wen X, Wang Q et al (2008) Environmental controls over carbon exchange of three forest ecosystems in eastern China. Global Change Biology 14(11):2555–2571. https://doi.org/10.1111/j.1365-2486.2008.01663.x

Yu G, Chen Z, Piao S, Peng C, Ciais P, Wang Q, Li X, Zhu X (2014) High carbon dioxide uptake by subtropical forest ecosystems in the East Asian monsoon region. Proc Natl Acad Sci U S A 111(13): 4910–4915. https://doi.org/10.1073/pnas.1317065111

Zhang S, Yu T, Li F, Wang X, Wang X (1985) The seasonal variations of area and intensity of polar vortex in Northern Hemisphere and relationship with temperature in Northeast China. Chin J Atmos Sci 9(2):178–185

Zhang H, Gao S, Zhang Y (2006) The interdecadal variation of North Polar Vortex and its relationships with spring precipitation in China. Clim Environ Res 11(5):593–604

Zhang H, Jin R, Zhang Y (2008) Relationships between summer Northern Polar Vortex with subtropical high and their influence on precipitation in North China. J Trop Meteorol 24(4):417–422

Zhang G, Kang Y, Han G, Sakurai K (2011) Effect of climate change over the past half century on the distribution, extent and NPP of ecosystems of Inner Mongolia. Glob Chang Biol 17(1):377–389. https://doi.org/10.1111/j.1365-2486.2010.02237.x

Zhang Y, Zhang C, Wang Z, Chen Y, Gang C, An R, Li J (2016) Vegetation dynamics and its driving forces from climate change and human activities in the Three-River Source region, China from 1982 to 2012. Sci Total Environ 563:210–220. https://doi.org/10.1016/j.scitotenv.2016.03.223

Zheng Z, Zhu W, Zhang Y (2020) Seasonally and spatially varied controls of climatic factors on net primary productivity in alpine grasslands on the Tibetan Plateau. Glob Ecol Conserv 21. https://doi.org/10.1016/j.gecco.2019.e00814